



ISSN 2047-3338

# Modified Gabor Filter with Control Chart and Image Plots for Identifying Architectural Distortion of Mammogram Images

Abhijith Bailur<sup>1</sup>, Amit Kumar Pandey<sup>2</sup>, Amit Kumar Sharma<sup>3</sup>, Shona Saseendran<sup>4</sup>, Abhinav<sup>5</sup>

<sup>1,2,4,5</sup>Cardea Biomedical Technologies Pvt Ltd, New Delhi, India

<sup>3</sup>Indian Institute of Technology-BHU, Varanasi, India

<sup>1</sup>abhijit\_bailur@yahoo.co.in

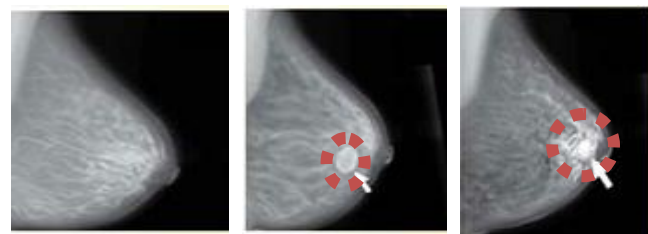
**Abstract**— Breast cancer is one of the fastest growing cancer and Architectural distortion is one of the important finding in the detection of cancer. The objective of this work is to develop a method for detecting architectural distorted area. In order to identify Architectural Distorted area this paper presents a novel method to distinguish Architectural Distortion (AD) and Non Architectural Distortion (Non AD) of Mammogram images, for the development of an efficient system. Among various breast abnormalities, architectural distortion is the most difficult type of tumour to detect. The proposed method could be applied as a solution to reduce the chances of human errors. The algorithm begins with a modified Gabor filters and orientation filter for identifying tissue patterns. Each detected tissue pattern is characterized into AD and NON AD based on mesh plot and contour plot which clearly states the variation in texture. Further the obtained result of modified gabor filter is tested with control chart to examine the effect of the algorithm. Statistical Parameter result obtained from control chart, for pre and post application of algorithm have showed a significance demarcation between AD and NON AD and also has proven the efficiency of the algorithm. 28 images from MIAS database were tested, with an efficiency of 89.4 percent to distinguish between the AD and Non AD And thus results obtained are promising in comparison with the previously published work.

**Index Terms**— Architectural Distortion (AD), Non Architectural Distortion (Non AD), Mammogram, Orientation, Andrew plot, Mesh Plot, Contour Plot and Control Chart

## I. INTRODUCTION

**B**REAST Cancer is a type of cancer which generally originates from breast tissues, usually in the ducts (tubes that carry milk to the nipple) and lobules (glands that make milk). It occurs in both men and women though it has a high probability of occurrence in women and can prove to be fatal. Mammograms is a test performed [1] to carry out early onset of breast cancer and can prove to be a life saving and could reduce the mortality rate. But architectural Distortion is one of the commonly missed signs which could be very fatal [2]. Each year almost 24,000 women under the age 45 are diagnosed with cancer in the United States [3]. Over 100,000 new breast cancer patients are estimated to be diagnosed

annually in India [4]. Breast cancer cases are expected to increase by 26% by 2020 and most of these will be seen in developing countries [5]. Breast cancer incidence and death rates generally increase with age with Ninety-five percent of breast cancer deaths occurring in women with 40 years of age and older in United States [6]. Diagnosing error which could be a result in human error can lead to abnormality being undetected. Around 50,000 to 90,000 American Women are being Incorrectly Diagnosed with Breast Cancer Annually [7]. Good skill and experience is needed in understanding the complex problem which is generally encountered in diagnosing cancer, so developing new ways in terms Computer aided diagnosis to limit the errors is a priority. In Fig. 1, we can see mammogram images varying from normal, benign to malignant respectively.



(a): Normal

(b): Benign

(c): Malignant

Fig. 1: Mamogram Images

Initial screening is always carried out by Mammography, although there are many others. All women who are having a suspect of cancer go through mammography screening procedures. Early confirmation leads to an effective and better plan of action for treatment. Various algorithms are developed to aid radiologist to provide a second opinion and the final decision is left to the radiologists. A mammogram image typically shows variation in gray levels of contrast inside the breast which would characterize normal tissue or the presence of calcification and masses. Oriented texture pattern which typically converges toward the nipple in case of normal images, is distorted in the presence of architectural distortion

[8]. No definite mass is visible in case of architectural distortion. Microcalcifications, circumscribed masses, spiculated masses and architectural distortions are some of the signs always a radiologist look for [9] which would play a significant role in deciding the condition of the patient. Fig. 2 describes different variants like Architectural Distortion, Spiculated Mass, Micro-calcification & Circumscribed mammogram images are shown in Fig. 2(a) to Fig. 2(d) respectively.

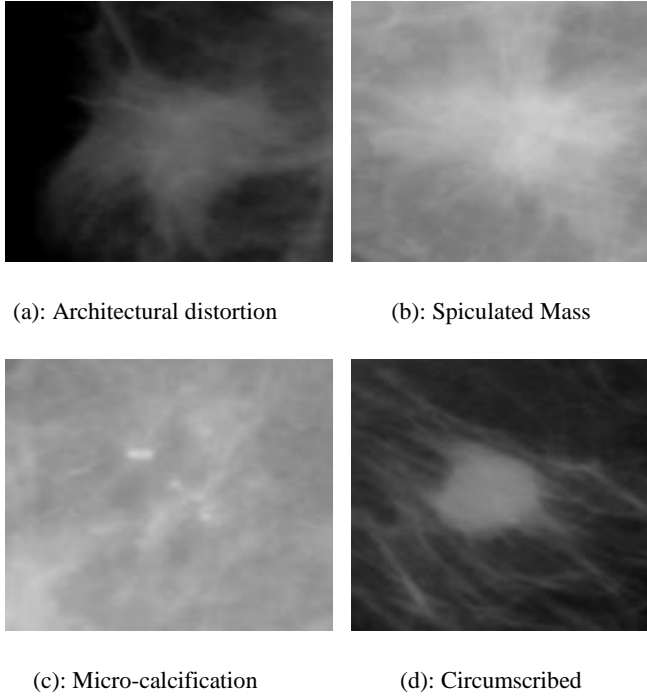


Fig. 2: Mamogram Region of Interest

Several algorithm for Discrimination and classification of mammograms with definite mass for benign, malignant and normal tissues [10] have been carried out. An architectural distortion is the one with no definite mass visible [11] hence making it the most difficult type of tumour to detect and it is a third most-common appearance of breast cancer [12]. Computer aided diagnosis method using Gabor filters [13], [14], phase portrait [14] analysis, fractal analysis [15], and texture analysis [16], [17], [18] are mainly used applied for mammogram images. Gabor filters and phase portrait maps [14], [19], [20], [21] to characterize oriented texture patterns in mammograms to detect architectural distortion have been discussed vastly.

A method based on statistical analysis of pixel orientation [22], where increase in pixels pointing to a region is found based on which the pixels are marked suspicious. Also a technique for the enhancement of spiculations in which a linear filter is applied to the Radon transform of the image. The enhanced image is filtered with radial spiculation filters to detect speculated masses and architectural distortion [23]. Though these approaches were effective for the estimation of

architectural distortion, the complexity observed is higher in those algorithms. A need is felt to develop low complex algorithm for the estimation of architectural distortion. So the objective was to develop a method which would clearly state the difference between AD and NON AD region graphically and statistically. We believe that AD region is made up of a cluster of structure resembling like a line with different orientations. So the method discussed can be summarized under four stages one with extraction of ROI with potential Ads and NON AD's, the second stages is implementation of Gabor filters the next stage is recognition of potential ADs using spectral variation, contour plot and Andrew plot with graphical result and also statistical result by the use of Contour plot. The final fourth stage would comprise of providing a comparative result between AD and NON AD region and to check the efficiency of algorithm results were shown prior and post application of algorithm. Our work shows a significance variation of spectral variation as observed through mesh plot and also a volume of distribution using contour plot as compared to the previously published result [11]. A new approach using Andrew plot and control chart is being introduced which provides a significant influence to the objective of the work which has been discussed in the result section.

## II. METHODOLOGY

### A. Preprocessing

The region of interest is defined by x and y co-ordinate with r the radius by radiologist in the MIAS database, which resembles a circular region of interest. For implementing the objectives of the work, a circular co ordinate needs to be converted into a rectangular coordinate which can be extracted. Refer to (1) which will approximately cover the area of interest as defined by the radiologist. This co-ordinate area is used to extract Architectural distorted area ( $I_{AD}$ ) using the inbuilt function of Matlab® where as for extracting Non Architectural distorted area ( $I_{NonAD}$ ) refer (2).

$$I_{AD} = [x - r, 1000 - y, 2r, 2r] \quad (1)$$

$$I_{NonAD} = [x + 50 - r, 900 - y, 2r, 2r] \quad (2)$$

The image can then be resized to 128 x 128, 512 x 512, and 256 x 256. In this work the ROI were resized to 128 X 128.

### B. Final Stage

Entropy is a statistical measure of the degree of randomness that can be used to characterize the texture of the input image. During Architecture Distortion the oriented features changes the normal pattern. There is a possibility that entropy might also change. If the pattern is that of a normal ROI then it does not have much impact on the outcome. In short if there is uncertainty in the images then it can be found. Equation (3)

defines Entropy of 1D data where  $P(X_j)$  is the Probability mass distribution.

$$E(x) = - \sum_{j=1}^k P(X_j) \log P(X_j) \quad (3)$$

For a 2D array refer (4), here  $P$  is the intensity in

$$E(I) = - \sum_{j=1}^m \sum_{j=1}^n \text{hist}_N(P) \log(\text{hist}_N(P)) \quad (4)$$

$m \times n$  image  $I(i, j)$  and  $\text{hist}_N(P)$  is the histogram properly normalized. Literature surveys also reveal that entropy has a significant role in affecting the signs of neoplasm in breast [24-26]. So the entropy was removed from all the ROI to prepare the data sets for further processing.

### C. Gabor filtering for Orientation field

The AD lines are straight lines hence are not oriented towards the nipple and do not have angular edges. Because of the orientation of normal tissue structures, radiologists generally conclude that AD regions are not clear. Finding the exact position of AD is important as this lesion is always identified as BIRADS category 4 or category 5 [27]. This has led to a challenge of determining oriented structure in image. Gabor filter is very significant in determining the oriented texture. Numerous works have been carried out and shown the benefits of Gabor Filter [28] - [30]. To extract the texture in a mammogram, the filtered image of the previous stage is allowed to run over a bank of Gabor filters for specific orientations [28]. Gabor filter is justified due its good detection with an accuracy of linear patterns. The Gabor filter kernel is given by eqn (6). The  $S_x$  and  $S_y$  are variance along  $x$  and  $y$  axis,  $\theta$  represent orientation and  $f$  is the frequency. The values of  $S_x$ ,  $S_y$  and  $f$  were chosen empirically. Gaussian kernel is used generally for weighting neighbors by their proximity to the pixel of interest and Fourier kernel is Fourier kernel provides us information about patterns in the image, when these two kernels are taken together we obtain the Gabor filter:

$$\text{GaborFit}(\sigma, \omega, \theta) = \text{GaussKernel}(\sigma) * \text{FourierKernel}(\omega, \theta) \quad (5)$$

$$E_i(x, y) = \left[ \frac{1}{2 \times \pi \times S_x \times S_y} \times \exp \left[ \frac{-1}{2} \left( \left( \frac{x}{S_x} \right)^2 + \left( \frac{y}{S_y} \right)^2 \right) \right] \right] * M_i(x, y, f) \quad (6)$$

$i=1,2;$

$$M_1(x, y, f) = \text{Cos} \left( 2 * \pi * f * \left( \left( \frac{\sqrt{x^2 + y^2}}{\sqrt{x^2 - y^2}} \right) \right) \right) \quad (7)$$

$$M_2(x, y, f) = \text{Cos}(2 * \pi * f * (x * \text{Cos} \theta + y * \text{sin} \theta)) \quad (8)$$

The values of  $S_x$ ,  $S_y$  and  $\theta$  justified for this work were finalized on the basis of trial and error. For determining the orientation in all direction, angles were changed in a set of six.

Orientations are obtained by varying angle  $\theta$  from 0, 30, 45, 60, 90 to 180 degrees. The output obtained at different angles corresponds to a particular image. Keeping this fact in mind that Gabor filter acts in different manner over the normal portions and over the abnormal patterns the results were computed for both the normal ROI and abnormal ROIs. The results were analyzed between before applying Gabor filter and after Gabor filter as the impact of Gabor filter has to be studied on both types of regions. The output of Gabor filter that is output of  $G_1$  and  $G_2$  were modified empirically to obtain the result as desired for AD and Non AD region refer (9) to refer (12). The output of the image obtained from equation (12) is similar to the size of the original extracted region.  $N_{Ga}$  and  $N_{Gam}$  are the number of samples from  $G_a$  and  $G_{am}$  respectively.

$$G_a = \frac{G_1}{G_2} \quad (9)$$

$$G_{am} = \frac{1}{N_{Ga}} \sum G_a \quad (10)$$

$$V = \frac{1}{N_{Gam}} \sum G_{am} \quad (11)$$

$$I = \frac{G_a}{V} \quad (12)$$

### D. Orientation Field and its importance

The orientation can be extracted from the Gabor filter but to find the variation in this output, to distinguish between distorted and non-distorted region, directional filters are used. Directional filters are nothing but banks of filters with different orientation. This filter processes the data as per the direction coefficient specified. We can easily find a distinction in such a case where we have an architectural variation from the obtained output. Using Gabor wavelets at different orientation and frequencies, Loan Buciu Alexandru Gascai [31] have described an approach where mammogram sample is filtered and directional features are extracted. Roberto H.Bamberger and Mark J.T.Smith [32] were the pioneers in directional filter estimation (DFE) for image processing which estimates directional flow and the filter has overcome the limited directional selectivity of separable wavelets. It finds its application in various imaging applications such as texture classification [33], image denoising [34], fingerprint image enhancement and recognition [35].

## III. PROPOSED NEW ALGORITHM

Following the previous available algorithm, a new efficient and an efficient decision making algorithm is proposed. Matlab® is utilized to implement. The following steps were followed to obtain the desired objective:

Step 1: Load the image.

Step 2: Refer (1) to extract the AD region of the image.

Step 3: Refer (2) to extract the NON AD Region of the image for optimizing our method by comparing AD & NON AD region.

Step 4: Pre-processing of Image - Resizing, Gaussian filter implementation (to remove Low component frequency) and Entropy Filtration refer (4).

Step 5: Equation (5) to Equation (8) for Gabor Filter Implementation

Step 6: Equation (9) to Equation (12) is completely a novel approach derived, scope of the equations is to visualize variation in the desired pattern.

Step 7: Visualize the output using Mesh plot, Andrew plot and contour plot for both AD and NON AD.

Step 8: The parameters obtained as an output of Control Chart is used to distinguish AD and NON AD numerically

#### IV. SIMULATION AND EVALUATION

This study used here discusses a novel approach for the classification of AD and Non AD regions. For AD and NON AD, two methods were used to show the results. One is a graphical output and other is a theoretical output. In this study, all ROIs within Mammogram images were chosen from MIAS database, and features for ROIs were analyzed and calculated. Images were analyzed with AD and NON AD. Results of the most efficient Gabor filter parameters chosen as  $\lambda = 8$ ,  $\theta = \pi/2$ ,  $\gamma = 1.5$ ,  $\text{band width} = 1$  &  $\text{Neighborhood} = 8$  is shown in Fig. 7. The output was then visualised using Andrew plot, Mesh plot & Contour plot and the plots were verified before applying algorithm for AD and Non AD. On analyzing the results there is a significant influence of the proposed algorithm on AD images. Andrew plot which observes the variation as a defined for the  $i$ -th observation of the ROI we could observe a subtle variation in the AD region due to the presence of change in orientation as shown in Fig. 3. When results obtained from Control Chart were analyzed, a range could be observed for  $\mu$  and  $\sigma$ , which are the constant parameters obtained from the control chart. Table 1 and Table 3 shows the result for  $\mu$  and  $\sigma$  on AD and NON AD images before and after applying algorithm. The average statistical response for  $\mu$  on applying algorithm will lie in the range of  $10.264 \pm 3$  for AD and for NON AD it is  $3.197 \pm 3$ . For  $\sigma$  the statistical data response was  $5.81 \pm 3$  for AD image and same for NON AD was  $0.03215 \pm 1$ .

Contour Plot as shown in Fig. 4 shows a significant distribution after applying the algorithm, due to variation in orientation less contour mass is observed. Similarly for mesh plot as in Fig. 5 and Fig. 6 we could observe a very less spectral density with spikes observed irregularly where as for the Non Ad region spectral variation could be seen evenly distributed. Y axis and X axis represents the image size from 1: rows to 1: columns of Image respectively and the Z axis represents single-valued function defined over a rectangular grid. Color represented is proportional to surface height.

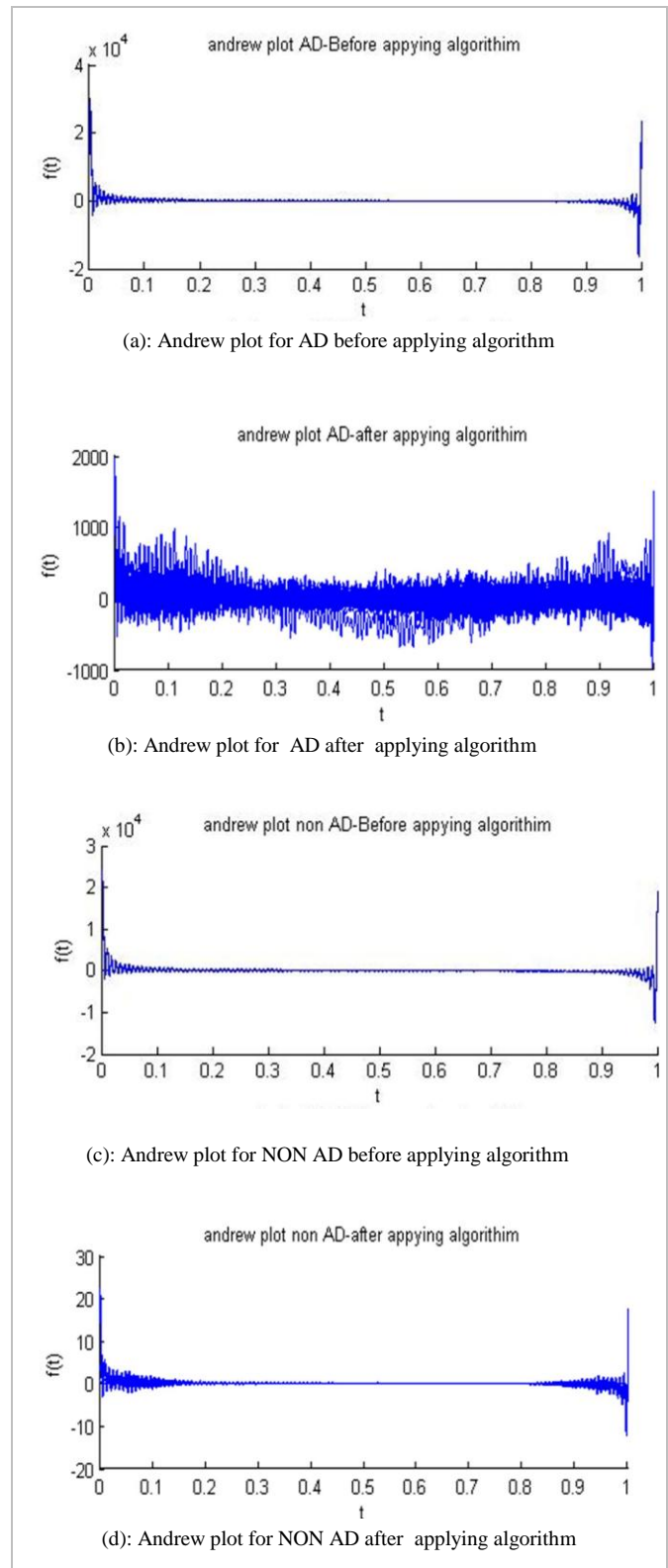
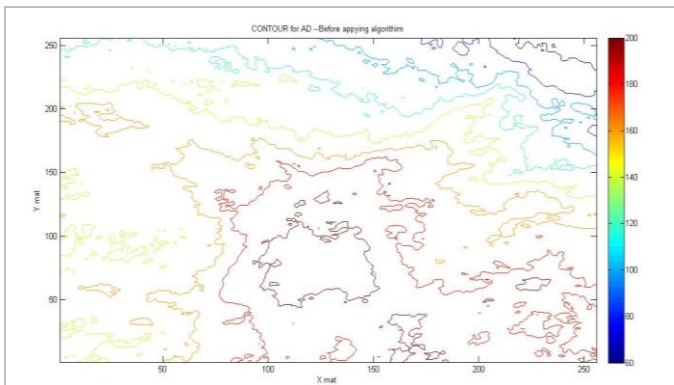
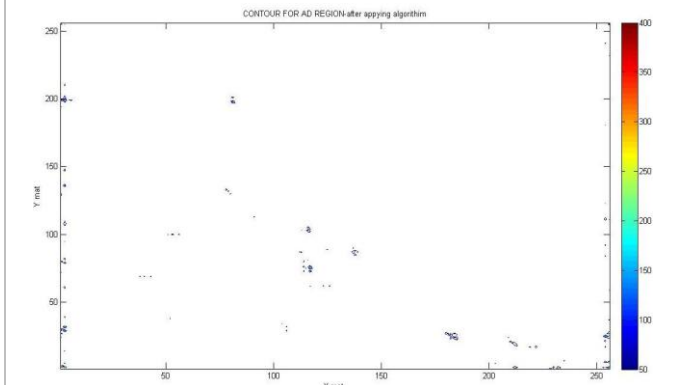


Fig. 3: Andrew Plot Before and After Applying Algorithm

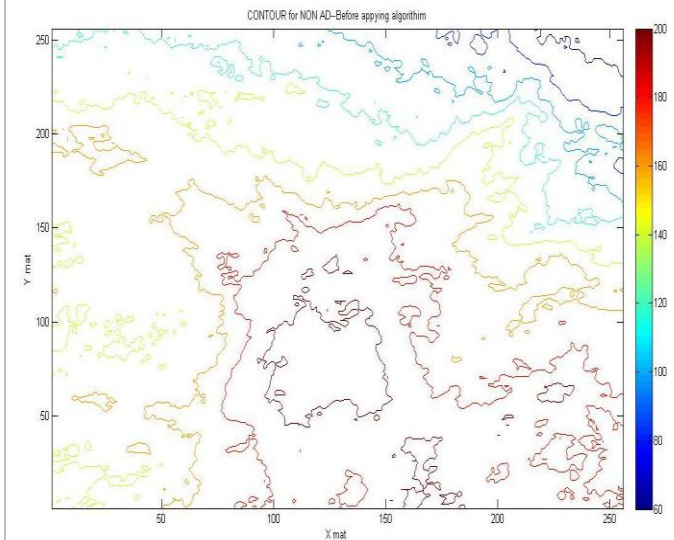
For evaluating the efficiency of algorithm two parameters were looked upon one being the computation time and the other was the efficiency to detect false images, from a set of 128 images, The average computation time observed was 8.34



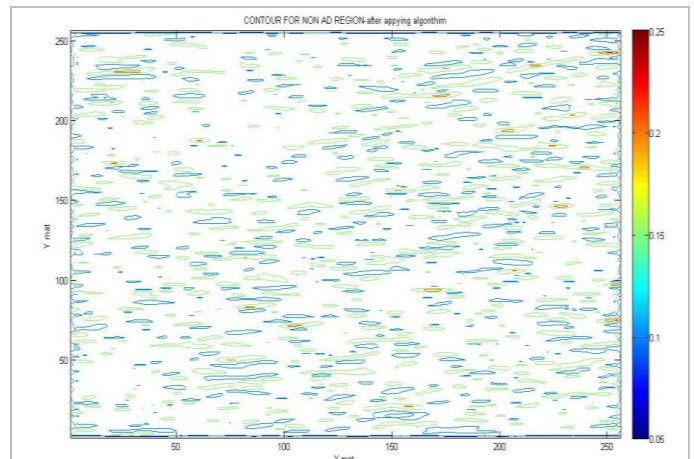
(a): Contour plot for AD before applying algorithm



(b): Contour plot for AD after applying algorithm



(c): Contour plot for NON AD before applying algorithm



(d): Contour plot for NON AD after applying algorithm

Fig. 4: Contour Plot Before and After Applying Algorithm

seconds. For the second parameter the test was performed on AD region where in 16 data sets were used out of which 14 data were recognized as AD images and a accuracy of 89.4 percent accuracy was observed for a data set of 19 non AD images, then finally the test data of 19 non AD images were mixed with 12 new AD images, all 12 were identified as AD and 17 were identified as Non AD with all the three plots and control chart parameters Mu and Sigma providing a clear result. Remaining two provided a satisfactory result for Mu, Sigma, and Andrew plot whereas clear differentiation could not be observed for mesh and Contour plot and the classification were manually observed for all the three plots.

TABLE I: CONTROL CHART PARAMETERS MU AND SIGMA BEFORE AND AFTER APPLYING ALGORITHM FOR “AD IMAGES”

Image Sets	Mu		Sigma	
	Before	After	Before	After
006	53.525	8.219	29.659	6.2186
013	163.827	7.648	63.738	5.8456
032	153.525	7.791	87.659	5.8942
039	132.642	7.981	43.789	4.8316
045	133.428	7.119	21.993	6.2913
074	169.731	15.603	61.191	3.1296
065	38.320	24.191	79.112	7.2542
103	112.691	6.981	91.321	7.1386
106	93.511	8.193	27.051	9.1662
113	213.021	9.149	41.104	4.2193
117	113.005	7.101	89.329	4.8149
123	196.249	13.201	57.711	4.9913

TABLE II: CONTROL CHART PARAMETERS MU AND SIGMA BEFORE AND AFTER APPLYING ALGORITHM FOR “NON AD IMAGES”

Image Sets	Mu		Sigma	
	Before	After	Before	After
002	49.228	9.1217	80.768	0.0186
007	154.702	0.1216	74.116	0.0296
011	150.818	0.1284	67.188	0.0459
020	161.228	0.1252	56.802	0.0346
031	61.121	9.0007	68.148	0.0186
049	159.872	0.1969	84.196	0.0296
062	170.911	0.1940	77.189	0.0459
088	139.288	0.1121	41.931	0.0346
091	63.110	8.9218	40.168	0.0186
100	54.793	10.126	71.116	0.0296
119	97.129	0.1916	56.190	0.0459
127	161.018	0.1249	60.179	0.0346

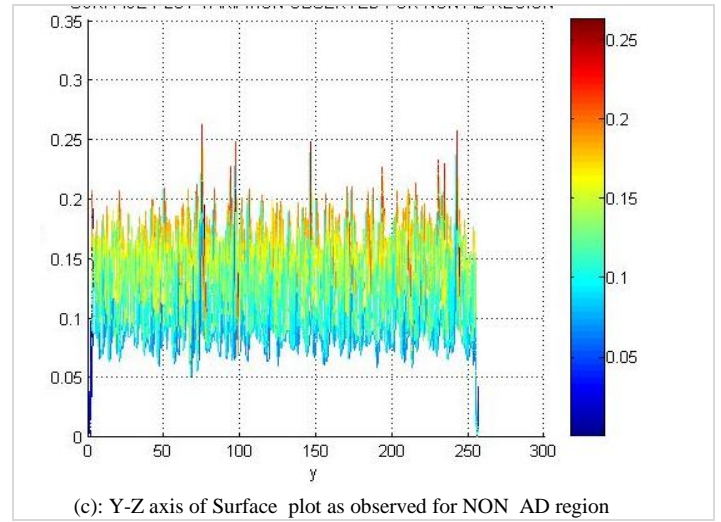
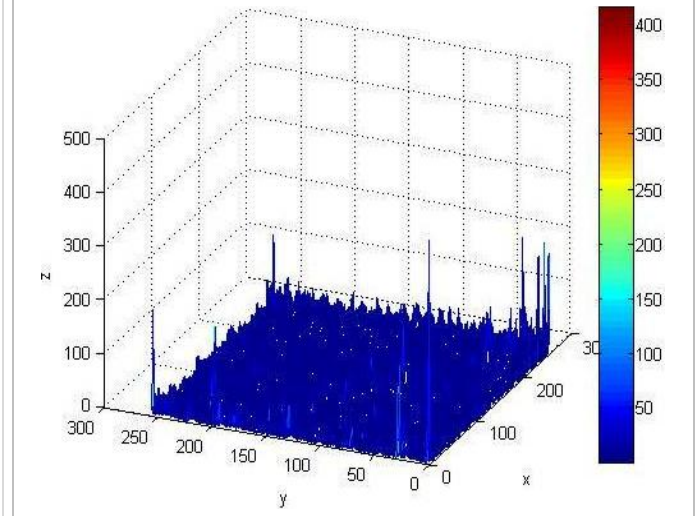
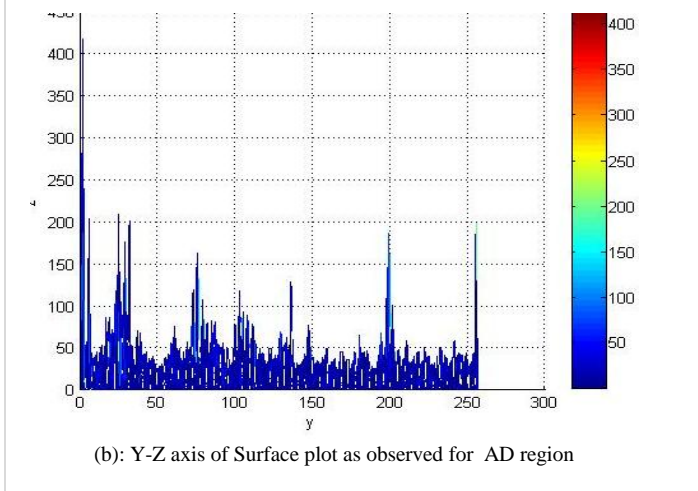
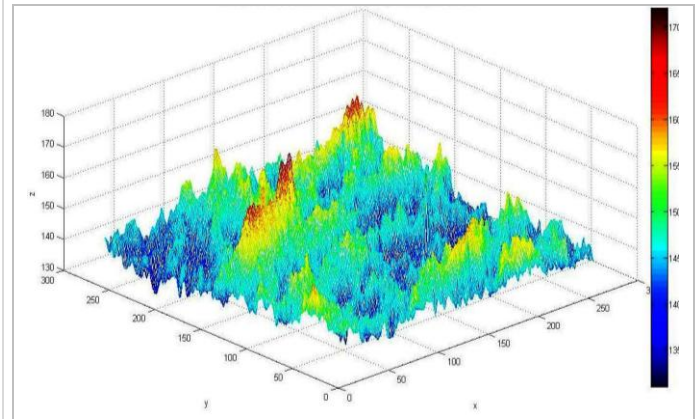
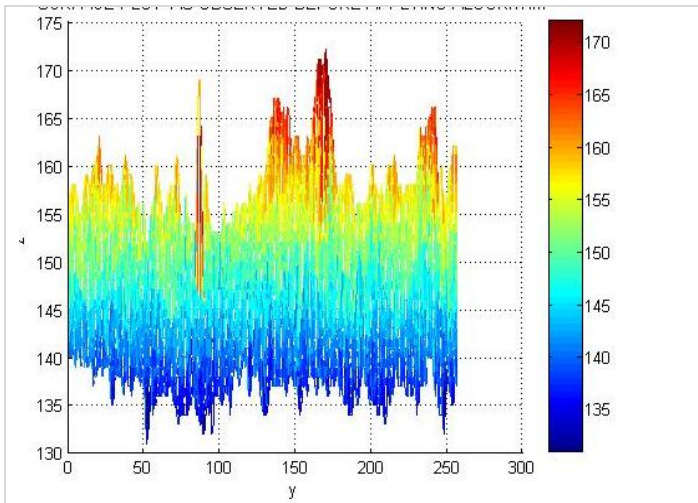


Fig. 5: Y-Z Axis View of Spectral Plot



## V. CONCLUSION

This paper presents a novel approach for the classification of AD and Non AD regions through graphs, image plots and numerical values by drawing Andrew plot, Mesh Plot, Contour Plot and by Control chart. Since architectural distortion is the most difficult type of tumour to detect, A new novel method of MU , Sigma and Andrew plot will definitely help radiologists to identify and distinguish AD from Non AD region with confidence and hence reduce the human errors substantially. The potential algorithm has to be studied on other available database. It would also be interesting to combine this algorithm on already available Computer diagnosis systems.

## REFERENCES

- [1] Dr. Samir Kumar Bandyopadhyay, Diagnosis of Breast Abnormalities in Mammographic Image, International Journal of Computer Science and Technology, March 2011. 2(1):69-71.
- [2] Magdalena Jasionowska, Artur Przelaskowski, Aleksandra Rutczynska, Anna Wroblewska. A Two-Step Method for Detection of Architectural Distortions in Mammograms. Information Technologies in Biomedicine Advances in Intelligent and Soft Computing ,2011. 69 : 73-84.
- [3] National Cancer Institute. Breast Cancer Treatment (PDQ®), Treatment Option Overview [Online]. Available: <http://www.cancer.gov/cancertopics/pdq/treatment/breast/Patient/page5>. [2013, September 20].
- [4] Murthy NS, Agarwal UK, Chaudhry K, Saxena S (2007). A study on time trends in incidence of breast cancer – Indian scenario. Eur J Cancer Care, 2007. 16: 185-1866.
- [5] Anita Khokhar, Breast Cancer in India: Where Do We Stand and Where Do We Go. Asian Pacific J Cancer Preview, 2012. 13 (10):4861-4866
- [6] American College of Radiology (ACR), Illustrated Breast Imaging Reporting and Data System (BI-RADS), 3rd ed. Reston, VA: Amer. Coll. Radiol, 1998
- [7] M. Elter, R. Schulz-Wendtland and T. Wittenberg .The prediction of breast cancer biopsy outcomes using two CAD approaches that both emphasize an intelligible decision process. Medical Physics , American Association of Physicists in Medicine , 2007. 34(11): 4164-4172.
- [8] Rita Filipa dos Santos Teixeira . Computer analysis of mammography images to aid diagnosis, MSc in Biomedical Engineering, Faculdade de Engenharia da Universidade do Porto , July 2012.33-35.
- [9] Stelios Halkiotis, Taxiarchis Botsis, Maria Rangoussi. Automatic detection of clustered microcalcifications in digital mammograms using mathematical morphology and neural networks, Journal of Signal Processing, July, 2007. 87 (7): 1559-1568.
- [10] M. Arfan Jaffar, Nawazish Naveed, Sultan Zia, Bilal Ahmed and Tae-Sun Choi. DCT features based malignancy and abnormality type detection method for mammograms, International Journal of Innovative Computing, Information and Control, September 2011,7(9) : 5495–5513.
- [11] Amit Kamra, Sukhwinder Singh and V K Jain. Towards the Detection of Architecture Distortion in Mammograms: A Review. International Journal of Computer Applications. Foundation of Computer Science, New York, USA. May 2012. 46(7):44-49.

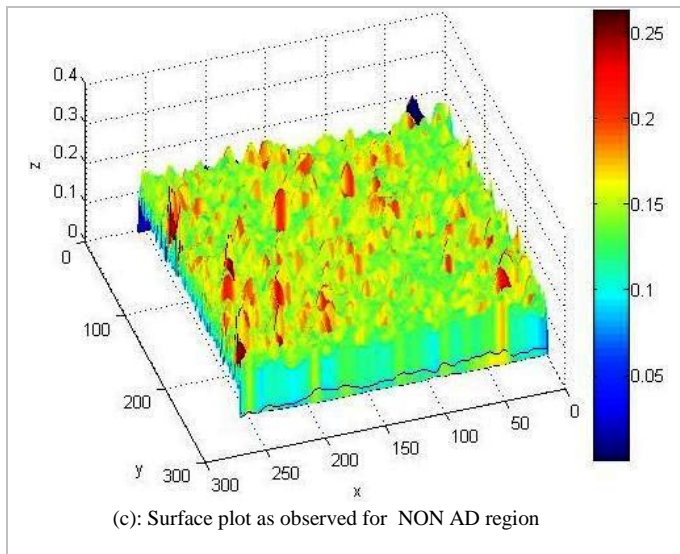


Fig. 6: Three Axis View of Spectral Plot

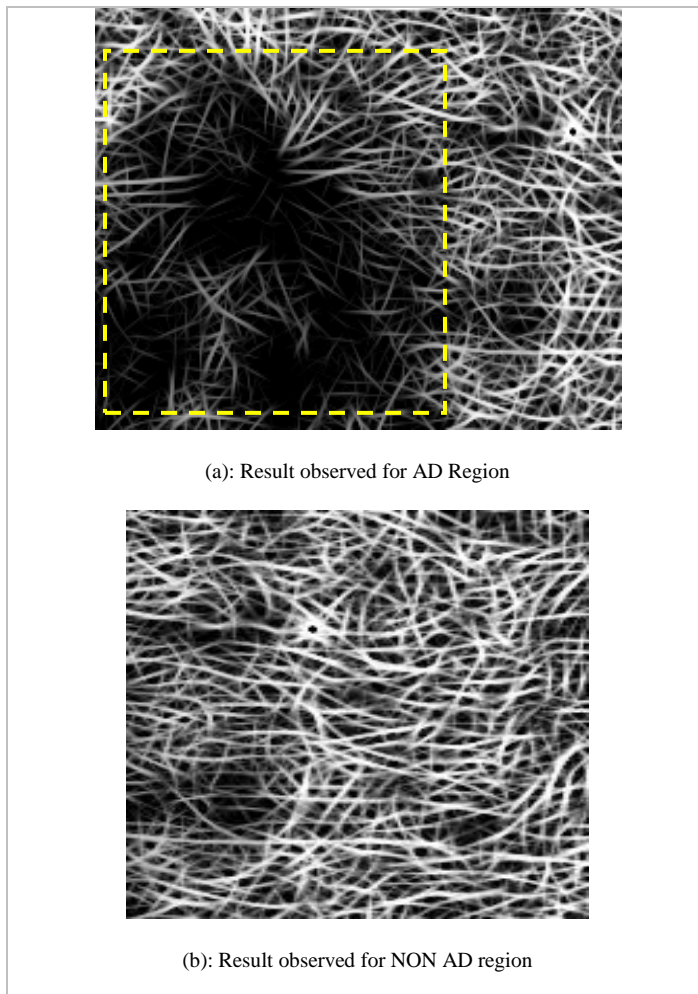


Fig. 7: Result Observed for Implementation of Step 6 in Section III

- [12] Shaheen R, Schimmelpenninck CA, Stoddart L, Raymond H, Slanetz PJ. Spectrum of diseases presenting as architectural distortion on mammography: multimodality radiologic imaging with pathologic correlation. *Pubmed US National Library of Medicine National Institutes of Health Semin Ultrasound CT MR* ,Aug 2011.32(4):351-62.
- [13] O'tega Ejofodomi , Michael Olawuyi, DonUche Onyishi , Godswill Ofualagba Detecting Architectural Distortion in Mammograms Using a Gabor.in: Harris Papadopoulos(ed), Andreas S Andreou(ed), Lazaros Iliadis(ed) and Ilias Maglogiannis(ed). *Artificial Intelligence Applications and Innovations*. Springer Berlin Heidelberg, 2013, 328-335.
- [14] R. M. Rangayyan and F. J. Ayres. Gabor filters and phase portraits for the detection of architectural distortion in mammograms. *Medical and Biological Engineering and Computing Journal* , 2006. 44(10): 883–894.
- [15] Rangaraj M. Rangayyan, Thanh M. Nguyen. Fractal Analysis of Contours of Breast Masses in Mammograms. *J Digit Imaging*, September 2007. 20(3): 223–237.
- [16] Rangaraj M. Rangayyan, Shantanu Banik, and J. E. Leo Desautels . Computer-Aided Detection of Architectural Distortion in Prior Mammograms of Interval Cancer. *Journal of Digital Imaging*. October 2010, 23(5) : 611-631.
- [17] Biswas, S.K.; Mukherjee, D.P., Recognizing Architectural Distortion in Mammogram: A Multiscale Texture Modeling Approach with GMM. *IEEE Transactions on Biomedical Engineering*, July 2011 . 58(7):2023-2030.
- [18] S Anand and Aynesh Vijaya R Rathna. Architectural Distortion Detection in Mammogram using Contourlet Transform and Texture Features. *International Journal of Computer Applications* ,Published by Foundation of Computer Science, New York, USA,July 2013.74(5):12-19
- [19] Ayres F.J, Rangayvan R.M. Characterization of architectural distortion in mammograms. *IEEE Engineering in Medicine and Biology Magazine*,Jan-Feb 2005.24(1):59-67.
- [20] F. J. Ayres and R. M. Rangayyan. Reduction of false positives in the detection of architectural distortion in mammograms by using a geometrically constrained phase portrait model. *International Journal of Computer Assisted Radiology and Surgery*, 2007. 1(6): 361–369.
- [21] Rangayyan, R. M., Banik, S., Desautels, J. L. Detection of Architectural Distortion in Prior Mammograms via Analysis of Oriented Patterns. *Journal of Visualized Experiments*. 2013 (78), doi: 10.3791/50341.
- [22] ] Karssemeijer N, Brake G.M. Detection of stellate distortions in mammograms. *IEEE Transactions on Medical Imaging*, October 1996. 15(5):611-619.
- [23] Mehul P. Sampat , Gary J. Whitman , Mia K. Markey , Alan C. Bovik. Evidence based detection of spiculated masses and architectural distortions. *Proc. SPIE 5747, Medical Imaging: Image Processing*, May 26 2005
- [24] Simon Marcellin , Djamel A. Zighed , and Gilbert Ritschard. Detection of breast cancer using an asymmetric entropy measure,Alferdo Rizzi (ed), Maurizio Vichi(ed). *Symposium Proc of Computational Statistics COMPSTAT* ,Physica-verlag –A Springer company,Rome-Italy, 2006. 975-982.
- [25] Rodrigues P.S, Giraldi G.A, Ruey-Feng Chang, Suri J.S. Non-Extensive Entropy for CAD Systems of Breast Cancer Images. *SIBGRAPI '06. 19th Brazilian Symposium on Computer Graphics and Image Processing*, October 2006. 8 (11) : 121-128.
- [26] Radu Mutihac, Alberto A Colavita, Andres Cicuttin, Alberto E Cerdeira. Maximum Entropy Improvement of X-Ray Digital Mammograms. in: Nico Karssemeijer (ed), Martin Thijssen(ed), Jan Hendriks(ed), Leon Erning(ed). *Digital Mammography: Computational Imaging and Vision*. Springer, Netherlands,1998.13:329-336.
- [27] Margaret M. Eberl, Chester H. Fox, Stephen B. Edge, Cathleen A. Carter, Martin C. Mahoney. *BI-RADS Classification for Management of Abnormal Mammograms*. *PubMed US National Library of Medicine National Institutes of Health* , March-April 2006 .19( 2): 161-164.
- [28] M. R. Turner. Texture discrimination by Gabor functions. *Biological Cybernetics*, 1986 . 55: 71–82.
- [29] A.K. Jain and F. Farrokhnia. Unsupervised texture segmentation using Gabor filters. *Pattern Recognition*, 1991. 24(12): 1167–1186.
- [30] Chia-Hung Wei, Yue Li and Chang-Tsun Li. Effective Extraction of Gabor Features for Adaptive Mammogram Retrieval. *Conf Proc of IEEE on Multimedia and Expo*, July 2007 :1503-1506.
- [31] I. Buciu and A. Gacsadi. Directional features for automatic tumour classification of mammogram images. *Biomed Signal Process Control*, 2010. doi:10.1016/j.bspc.2010.10.003
- [32] ] Roberto. H. Bamberger and Mark. J. T. Smith. A filter bank for the directional decomposition of images: Theory and design. *IEEE Transactions on Signal Processing*, 1992. 40(7):882-893.
- [33] T. Chen and P. Vaidyanathan. Considerations in multidimensional filter bank design. *Conf Proc of IEEE International Symposium on Circuits and Systems*, 5 may 1993. 643–645.
- [34] Y. P. Lin and P. P. Vaidyanathan. Theory and design of two-dimensional filter banks: a review. *Multidimensional Systems and Signal Processing*,1996. 7: 263–330
- [35] T. T. Nguyen and S .Oraintara. A Class of Multiresolution Directional Filter Banks. *IEEE Transactions on Signal Processing*, 2007. 55 (3):949-961.